

Dynamical spectra from one and two-photon Fock state pulses exciting a single chiral qubit in a waveguide

Sofia Arranz Regidor,^{1,*} Andreas Knorr,² and Stephen Hughes¹

¹*Department of Physics, Engineering Physics and Astronomy,
Queen's University, Kingston, Ontario, Canada, K7L 3N6*

²*Institut für Theoretische Physik, Nichtlineare Optik und Quantenelektronik,
Technische Universität Berlin, Berlin, 10623, Germany*

(Dated: October 8, 2024)

We study the dynamical light emission from few-photon Fock states in waveguide-QED with a chiral two-level system. We first investigate the time dynamics of the system by calculating the emitter population and illustrate the breakdown of the weak excitation approximation, for both 1-photon and 2-photon excitation. We show how a 1-photon pulse yields a transmitted long-time spectrum that is identical to the input pulse, despite significant population effects. However, the dynamical spectra and spectral intensity show rich population effects. We also show the differences between 1-photon and 2-photon excitation, where the latter shows clear signatures of nonlinear saturation effects. Analytical and numerically exact matrix product state solutions are shown.

Introduction.—The study of waveguide quantum electrodynamics (QED) has significantly improved our ability to control quantum light-matter interactions on chip, where quantum bits represented by two-level systems (TLSs) are coupled to a continuum of quantized field modes [1–18]. Waveguide photons coupled to atoms and resonant few-state systems present a fundamental model in quantum optics, and serve as a platform for emerging quantum optical applications [19–29].

Modelling quantized fields, for instance few photon states from waveguides interacting with TLSs presents a significant challenge, and often one adopts various approximations. For example, one can treat the waveguide as a *bath* that is subsequently traced out, or consider the system in a steady state (long time limit), or/and using a *weak excitation approximation* (WEA) where the TLSs remain unexcited. Often the WEA yields identical solutions to a quantized harmonic oscillator (HO) [30–32], but even at the single photon limit when involving finite electron population, the WEA can fundamentally break-down. There are established methods to model the exact few-photon transport in waveguide-QED, such as scattering solutions and input-output theories [33–37], which are convenient for computing long-time solutions. More direct dynamical approaches include time-dependent wavefunctions [4, 38], and Heisenberg treatments [39].

In this work, we study a quantum pulse containing only a few photons (one or two) interacting with a single chiral TLS in a waveguide (Fig. 1). To fully include the TLS dynamics and waveguide photons at the system level, we use matrix product states (MPS), an exact numerical method based on tensor network methods, which allows us to treat the TLS and the waveguide at the same level [40–44]. We complement our numerical approach by deriving analytical solutions for the TLS population for both a 1-photon and a 2-photon pulse. We also use MPS to obtain the time-dependent correlation functions and dynamical (time-dependent) spectra [39, 45, 46], and we

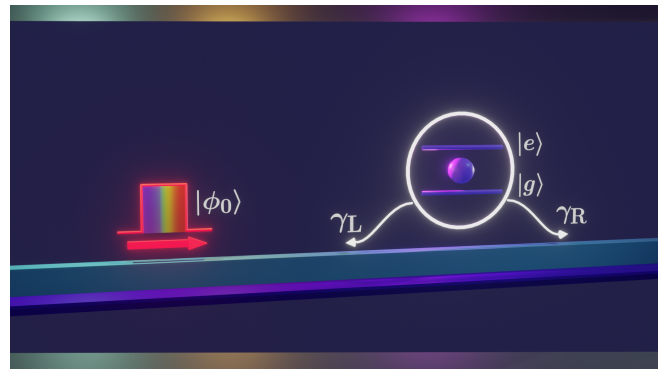


Figure 1. Schematic of a TLS coupled to an open waveguide, excited with an incident rectangular quantum pulse, which can be a 1-photon or 2-photon Fock (number) state.

derive the analytical solution of the correlation functions for the one-photon solution.

Based on this approach we gain several key insights: First, we investigate the time dynamics of the waveguide-TLS system, observing the breakdown of the WEA and clear TLS population dynamics, even for a single photon (as is well known [47]). Then we examine the transmitted spectra and observe that, strikingly, for 1-photon pulses, the TLS population effects are completely cancelled out in the long time limit for the transmitted spectrum. So how does one detect signatures of the population effects? We show how the time-dependent spectra and spectral intensity do contain signatures of the TLS population effects, showing significantly richer features than the usual CW resonance fluorescence features or the simple input spectrum of the pulse. For the 2-photon case, both the time-dependent spectra and the stationary (long time) spectra contain unique saturation effects, and show a significant spectral narrowing or reshaping. These results introduce a way to probe the intrinsic population and nonlinear effects that can occur in short-pulse dynamical

resonance fluorescence, and are timely with recent experiments in this regime, done so far with classical coherent fields [48, 49].

Theory.—We consider a chiral TLS that scatters to the right only, so $\gamma_L = 0$ and $\gamma = \gamma_R$ is the nominal decay rate. Symmetric emitter solutions are shown in Ref. 50. Using the equations of motion for the probability of the time-dependent atomic excitation amplitude of the TLS, we calculate the TLS population analytically [38, 39]. We consider the frequency center of the photon wave packet pulse and TLS on resonance, $\omega_p = \omega_0$, with the group velocity v_g (linear dispersion). We consider a square wave pulse shape, of width t_p . For the 1-photon (Fock state) pulse, we obtain the TLS population dynamics [50]:

$$\begin{aligned} n_{\text{TLS}}^{(1)}(t) &= \frac{4}{\gamma t_p} \left[e^{-\gamma t/2} - 1 \right]^2, & 0 \leq t \leq t_p, \\ n_{\text{TLS}}^{(1)}(t) &= \frac{4}{\gamma t_p} \left[1 - e^{\gamma t_p} \right]^2 e^{-\gamma t}, & t > t_p, \end{aligned} \quad (1)$$

and for the 2-photon pulse,

$$\begin{aligned} n_{\text{TLS}}^{(2)}(t) &= \frac{8}{\gamma t_p} \left[\left(\frac{-32}{\gamma t_p} + \frac{16t}{t_p} - 2 \right) e^{-\gamma t/2} - \frac{8}{\gamma t_p} + 1 \right. \\ &\quad \left. + \left(\frac{40}{\gamma t_p} + \frac{8t}{t_p} + 1 \right) e^{-\gamma t} \right], & 0 \leq t \leq t_p, \\ n_{\text{TLS}}^{(2)}(t) &= \frac{8}{\gamma t_p} \left[\left(\frac{-32}{\gamma t_p} + 14 \right) e^{\gamma t_p/2} + \left(\frac{-8}{\gamma t_p} + 1 \right) e^{\gamma t_p} \right. \\ &\quad \left. + \left(\frac{40}{\gamma t_p} + 9 \right) e^{-\gamma t} \right], & t > t_p. \end{aligned} \quad (2)$$

To obtain the full dynamical information for the quantum correlation functions and spectra, we use MPS [40].

The temporal shape of any general quantum pulse can be defined in the input creation operator b_{in}^\dagger , which creates the photons in the waveguide, $b_{\text{in}}^\dagger = \int dt f(t) b_R(t)^\dagger$, where $f(t)$ represents the pulse shape and $b_R(t)$ is the photon creation operator that creates a right moving photon at a time t . In the MPS description, this is discretized and introduced in the bosonic part of the input state. In the case of a single photon pulse, then

$$|\phi_0\rangle_N = \sum_{k=1}^N f_k \Delta B_k^\dagger / \sqrt{\Delta t} |0, \dots, 0\rangle, \quad (3)$$

where f_k is the discretized version of $f(t)$, and $\Delta B_k^\dagger = \int_{t_k}^{t_{k+1}} dt' b_R^\dagger(t')$ is the quantum noise operator [50].

Population dynamics and transmitted stationary spectra.—In Fig. 2, we study an incident rectangular pulse with a width of $\gamma t_p = 2$ (shaded region), containing either 1 photon [Fig. 2(a)] or 2 photons [Fig. 2(b)], interacting with the chiral TLS. The population dynamics

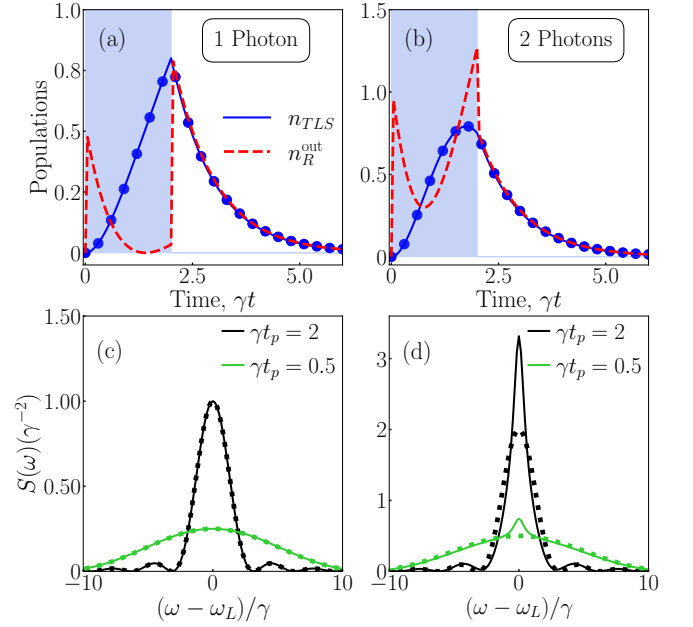


Figure 2. (a,b) Quantum dynamics for a chiral single TLS-waveguide system, using an incident rectangular quantum pulse (with duration $2\gamma^{-1}$, cyan shaded region) containing: (a) one photon, and (b) two photons. Both panels show the TLS population (solid blue), with the corresponding analytical solution (blue circles), and the normalized photon population of the right moving photons (dashed red). (c) Stationary spectrum, $S(\omega)$, for 1-photon with $\gamma t_p = 2$ (black solid line) and $\gamma t_p = 0.5$ (green solid line), and the corresponding solutions without the TLS interaction (dashed lines). (d) $S(\omega)$ for a 2-photon pulse, with similar labels to (c), where dashed lines show solutions without the TLS interaction.

are calculated analytically (blue circles) and using MPS (solid line), which show perfect agreement. The normalized photon population $n_R^{\text{out}} = \langle \Delta B_k^\dagger \Delta B_k \rangle / (\Delta t)^2$ is shown as well for the right-moving photons (dashed red).

For these relatively short pulses, we observe a high TLS population as the pulse interacts with the TLS, which then exponentially decays. These results completely deviate from the weak excitation regime, even in the 1-photon case, consistent with [47]. Furthermore, the TLS population is higher in the single photon case. This is due to a nonlinear feature in the 2-photon pulse solution, highlighting the complex nonlinear population saturation interactions with two photons. These population effects are further studied in Ref. 50, where the effects of pulse duration are investigated, showing significant TLS populations, greater than 0.1 for pulses as long as 100γ .

Figure 2(c) shows the input and transmitted 1-photon stationary spectrum for the same pulse duration as in (a) ($\gamma t_p = 2$) and for a shorter pulse duration of $\gamma t_p = 0.5$. For both pulse durations, all the population effects we observed in the TLS dynamical figures perfectly cancel out, i.e., the spectrum is insensitive to population dynamics. This is why a WEA solution can happen to give the same

result as a full TLS solution with dynamical excitation, even though a WEA assumption for the population is clearly not valid. However, this correspondence is not the case when the input pulse contains 2 photons, as shown in Fig 2(d), where the transmitted spectra is calculated again for a pulse durations of $\gamma t_p = 2$ and $\gamma t_p = 0.5$, and compared with the input pulse. Here, a clear nonlinear feature can be observed, where an additional peak with bandwidth γ appears at the central frequency, qualitatively differing from the input field spectra.

Analytical solution for the 1-photon long-time spectra.—In Fig. 2(c), we used MPS to compute the stationary spectra, and find that the transmitted spectrum is identical to the input spectra, even though Fig. 2(a) shows significant population effects. To help explain the absence of TLS population effects for the long-time spectra, in the case of 1-photon excitation, we can use the analytical methods in Ref. 50.

We consider a right-propagating 1-photon field $a_R(t)$, described through the boson operator, $a_{in}(t) = a_0 f(t)/\sqrt{v_g}$ containing the pulse shape $f(t)$ and the annihilation operator a_0 that annihilates a waveguide photon $a_0 |0\rangle = 0$. The transmitted spectrum $S(\omega)$ is

$$S(\omega) = v_g \left\langle \left(a_{in}^\dagger(\omega) - \frac{g_0^R}{v_g} \sigma^+(\omega) \right) \left(a_{in}(\omega) - \frac{g_0^R}{v_g} \sigma^-(\omega) \right) \right\rangle, \quad (4)$$

where $\langle a_{in}^\dagger(\omega) a_{in}(\omega) \rangle = |f(\omega)|^2$, $\sigma^{+/-}(\omega)$ are the raising and lowering operators for the TLS, and g_0^R is the (right travelling) photon-TLS coupling term. Solving Eq. (4) explicitly (full derivation in [50]), yields

$$S(\omega) = |f(\omega)|^2 - \frac{\gamma |f(\omega)|^2}{i(\omega - \delta) + \gamma} - \frac{\gamma |f(\omega)|^2}{-i(\omega - \delta) + \gamma} + \frac{\gamma^2 |f(\omega)|^2}{(\omega - \delta)^2 + \gamma^2} \equiv |f(\omega)|^2, \quad (5)$$

where $\delta = \omega_a - \omega_0$, with ω_a the TLS frequency. Thus, we simply obtain the incident pulse profile, and all TLS effects perfectly cancel out, in agreement with results shown in Fig. 2(c). Interestingly, Eq. (5) is valid for any pulse shape despite the fact that different $f(t)$ generate different pulse dynamics.

Dynamical spectra.—To better understand the time-dependent population dynamics and how it manifests in experiments, we define and connect to two dynamical observables that have also been probed in recent experiments [48, 49]: time-dependent (dynamical) spectra, $S(\omega, t)$ and frequency-dependent intensity, $I(\omega, t)$. In a rotating wave approximation, the transmitted *time-dependent spectrum* is obtained from

$$S(\omega, t) = \text{Re} \left[\int_0^t dt' \int_0^{t-t'} d\tau v_g \langle a_R^\dagger(t') a_R(t' + \tau) \rangle e^{i\Delta_{\omega p} \tau} \right], \quad (6)$$

where $\Delta_{\omega p} = \omega - \omega_p$. In the long time limit, when $t \rightarrow \infty$, we obtain $S(\omega) = S(\omega, t \rightarrow \infty)$. We stress that $S(\omega, t)$ contains features that are unique to the regime of *dynamical resonance fluorescence*.

For the same regime of pulsed excitations, we can also compute the emitted time-dependent spectral intensity,

$$I(\omega, t) = \text{Re} \left[\int_0^\infty d\tau v_g \langle a_R^\dagger(t) a_R(t + \tau) \rangle e^{i\Delta_{\omega p} \tau} \right], \quad (7)$$

and we note the interesting relationship: $S(\omega) = I(\omega) = \int_0^\infty I(\omega, t) dt$ [48], so the time-integrated spectral intensity is equivalent to the long-time spectra, but the dynamical signatures are quite different. We highlight that the time-dependent spectral intensity was recently measured in cavity-QED experiments with *classical* pulses [48], specifically with quantum dots in cavities, using an etalon filter and a fast photon detector.

Figure 3 shows the time-dependent spectra, $S(\omega, t)$, calculated using Eq. (6) for a pulse of length $\gamma t_p = 2$ containing 1 photon [Fig. 3(a)] and 2 photons [Fig. 3(c)]. Figure 3(b) represents the solution without the TLS for reference, which has naturally no population effects; note that neglecting population effects in the dynamical case leads to unphysical time-dependent spectra, $S(\omega, t)$, (which is negative), but identical stationary spectra. In addition, the TLS population is shown on the left to better understand the correlation with the population dynamics. *In this dynamical case, we can appreciate the time-dependent TLS population effects on the spectrum, even in the 1-photon solution, both during the pulse and after the pulse.* Additionally, we observe a more pronounced center peak in the 2-photon solution (compared to the 1-photon case), manifested by nonlinear effects.

The frequency-dependent spectral intensity [Eq. (7)] results are shown in Fig. 3(d,e,f), where again we show the interaction of the TLS with a 1-photon pulse, the reference pulse, and the interaction with a 2-photon pulse, respectively. Here, we observe a qualitatively different profile, as a function of time, as we now also probe part of the dynamics of the two-time photon correlation function. For instance, we can have positive and negative values, though in practice, actual measurements will yield a net positive quantity when using spectral filters [48]. Nevertheless, we again see clear TLS population effects in both the 1 and 2-photon solutions, with an enhancement of the central peak in the latter case. This is again observed in Fig. 4, with a longer pulse ($\gamma t_p = 10$), where both results show temporal dynamics. Now, we see how the 1-photon case has more subtle dynamics since the TLS population is smaller than with shorter pulses. However, in the 2-photon results, there is a clear nonlinear interaction showing a pulse break-up in frequency, consistent with results on collective chiral emitters [44].

We also see how the time-integrated intensity, $I(\omega)$, coincides with the stationary spectrum, $S(\omega)$ (solid green lines in Figs. 3 and 4), where the TLS population effects

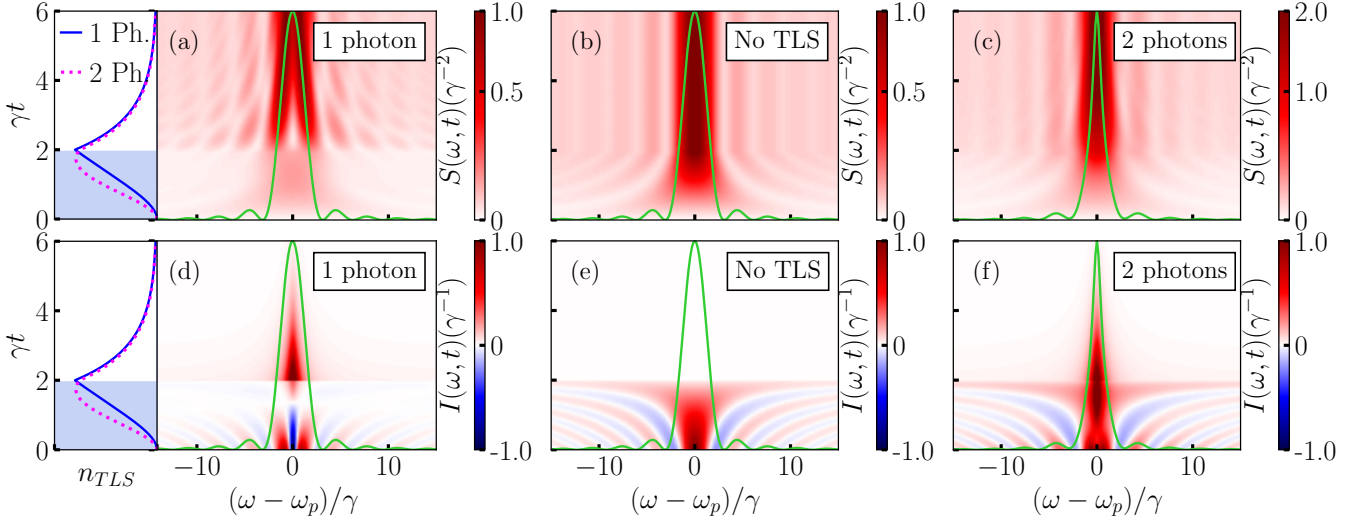


Figure 3. (a,b,c) Time-dependent spectrum, $S(\omega, t)$, of (a) a 1-photon and (b) a 2-photon pulse with a pulse length $t_p = 2/\gamma$ interacting with a chiral TLS, and (c) a 1-photon pulse of the same length without the TLS interaction. (d,e,f) Time-dependent spectral intensity, $I(\omega, t)$, of (d) a 1-photon and (e) a 2-photon quantum pulse with a pulse length $t_p = 2/\gamma$ interacting with a chiral TLS, and (f) a 1-photon pulse of the same length without the TLS interaction. The corresponding long time limit $S(\omega)$, is plotted in the six cases in green. On the left, the TLS population (n_{TLS}) is plotted for both the interaction with a 1-photon pulse (solid blue curve) and a 2-photon pulse (dashed magenta curve) and the pulse is shown with a blue shade.

are perfectly cancelled for the 1-photon pulse. Again, this feature is only true in the long time limit of Eq. (6); in contrast, the *time-dependent* spectra and intensity instead contain clear signatures of population effects even for 1 photon excitation. For 2 photon excitation, we also obtain nonlinear effects, both in the time-dependent spectral functions as well as the stationary spectra.

To gain further insight into the role of the population effects, we have derived an analytical solution for the relevant two-time correlation function (full derivation can be found in Ref. [50]). For example, when $t > t_p$, we have

$$v_g \langle a_R^\dagger(t) a_R(t + \tau) \rangle = \frac{4}{t_p} \left(e^{\gamma t_p/2} - 1 \right)^2 e^{-\gamma(t+\tau/2)}, \quad (8)$$

which uses the single-time solution as the initial condition, from ($t > t_p$)

$$v_g \langle a_R^\dagger(t) a_R(t) \rangle = \frac{4}{t_p} \left[e^{\gamma t_p/2} - 1 \right]^2 e^{-\gamma t}, \quad (9)$$

which closely resembles the population dynamics (see Eq. (1)), showing that population effects directly affect both $S(\omega, t)$ and $I(\omega, t)$. Thus, our results suggest that dynamical spectra can be used to measure dynamical TLS population effects with few photon sources.

Summary.—We have investigated the time dynamics of a chiral TLS in a waveguide when excited with a rectangular quantum pulse containing few photon excitations, specifically using an n -photon Fock state. We have shown how the WEA breaks down, and significant population features are observed with both 1- and 2-photon pulses.

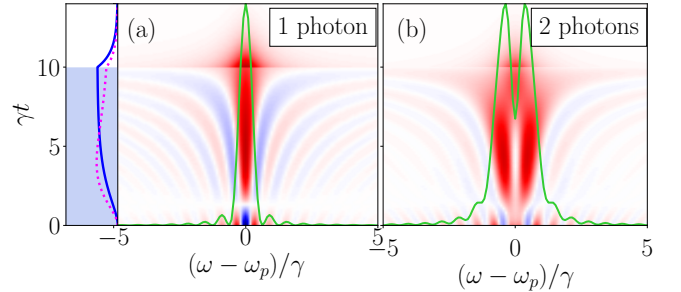


Figure 4. Time-dependent spectral intensity, $I(\omega, t)$, of (a) a 1-photon and (b) a 2-photon quantum pulse with a pulse length $t_p = 10/\gamma$ interacting with a chiral TLS. The corresponding stationary spectra $S(\omega)$, is plotted in green. On the left, the TLS population (n_{TLS}) is plotted for both the interaction with a 1-photon pulse (solid blue curve) and a 2-photon pulse (dashed magenta curve) and the pulse is shown with a blue shade.

For the case of 1 photon excitation, we have demonstrated how the TLS dynamical signatures cannot be observed in the stationary spectrum, since all the population effects cancel out in the long time limit. However, the impact of the population dynamics is readily shown in the dynamical spectral functions, for both $S(\omega, t)$ and $I(\omega, t)$, computed using a numerically exact MPS approach. These spectral observables represent dynamical solutions which notably contain population effects in the time-dependent spectrum solution. For 2-photon excitation, we showed how both the stationary and dynamical spectra contain rich population and nonlinear features.

Apart from fundamental quantum optics interest, our results also impact many current models in pulsed waveguide-QED systems with few photon sources, as the WEA is often adopted in many of the scattering theories; however, our predictions do not rely on any weak excitation assumptions, and our results are also timely with recent experimental works on measuring the *dynamical* resonance fluorescence regime [48, 49]. Finally, while our results were presented for a short rectangular pulse, our general conclusions and models can be extended to longer pulses, and for any quantum pulse shape, including Gaussian time profiles [50]. Indeed, we find that significant population effects occur even for relatively long pulses, with populations $N_{TLS} > 0.05$ for durations $t_p > 100/\gamma$ [50].

This work was supported by the Natural Sciences and Engineering Research Council of Canada (NSERC) [Discovery and Quantum Alliance Grants], the National Research Council of Canada (NRC), the Canadian Foundation for Innovation (CFI), Queen's University, Canada, and the Alexander von Humboldt Foundation through a Humboldt Award. We also thank Kisa Barkemeyer, Jacob Ewaniuk, and Nir Rotenberg for valuable contributions and discussions.

* 18sar4@queensu.ca

- [1] D. Witthaut and A. S. Sørensen, Photon scattering by a three-level emitter in a one-dimensional waveguide, *New Journal of Physics* **12**, 043052 (2010).
- [2] D. Roy, Two-photon scattering by a driven three-level emitter in a one-dimensional waveguide and electromagnetically induced transparency, *Phys. Rev. Lett.* **106**, 053601 (2011).
- [3] E. Sanchez-Burillo, D. Zueco, J. J. Garcia-Ripoll, and L. Martin-Moreno, Scattering in the ultrastrong regime: Nonlinear optics with one photon, *Phys. Rev. Lett.* **113**, 263604 (2014).
- [4] A. Nysteen, P. T. Kristensen, D. P. S. McCutcheon, P. Kaer, and J. Mørk, Scattering of two photons on a quantum emitter in a one-dimensional waveguide: exact dynamics and induced correlations, *New Journal of Physics* **17**, 023030 (2015).
- [5] P. Longo, P. Schmitteckert, and K. Busch, Few-photon transport in low-dimensional systems, *Phys. Rev. A* **83**, 063828 (2011).
- [6] S. Longhi, Rabi oscillations of bound states in the continuum, *Opt. Lett.* **46**, 2091 (2021).
- [7] I.-C. Hoi, A. F. Kockum, L. Tornberg, A. Pourkabirian, G. Johansson, P. Delsing, and C. M. Wilson, Probing the quantum vacuum with an artificial atom in front of a mirror, *Nature Physics* **11**, 1045–1049 (2015).
- [8] H. Pichler and P. Zoller, Photonic circuits with time delays and quantum feedback, *Phys. Rev. Lett.* **116**, 093601 (2016).
- [9] H. Zheng, D. J. Gauthier, and H. U. Baranger, Waveguide QED: Many-body bound-state effects in coherent and Fock-state scattering from a two-level system, *Phys. Rev. A* **82**, 063816 (2010).
- [10] B. Kannan, M. J. Ruckriegel, D. L. Campbell, A. Frisk Kockum, J. Braumüller, D. K. Kim, M. Kjaergaard, P. Krantz, A. Melville, B. M. Niedzielski, A. Vepsäläinen, R. Winik, J. L. Yoder, F. Nori, T. P. Orlando, S. Gustavsson, and W. D. Oliver, Waveguide quantum electrodynamics with superconducting artificial giant atoms, *Nature* **583**, 775–779 (2020).
- [11] B. Kannan, A. Almanakly, Y. Sung, A. Di Paolo, D. A. Rower, J. Braumüller, A. Melville, B. M. Niedzielski, A. Karamlou, K. Serniak, A. Vepsäläinen, M. E. Schwartz, J. L. Yoder, R. Winik, J. I.-J. Wang, T. P. Orlando, S. Gustavsson, J. A. Grover, and W. D. Oliver, On-demand directional microwave photon emission using waveguide quantum electrodynamics, *Nature Physics* **19**, 394–400 (2023).
- [12] P. Lodahl, S. Mahmoodian, S. Stobbe, A. Rauschenbeutel, P. Schneeweiss, J. Volz, H. Pichler, and P. Zoller, Chiral quantum optics, *Nature* **541**, 473 (2017).
- [13] D. Roy, C. M. Wilson, and O. Firstenberg, Colloquium: Strongly interacting photons in one-dimensional continuum, *Rev. Mod. Phys.* **89**, 021001 (2017).
- [14] P. Y. Wen, K.-T. Lin, A. F. Kockum, B. Suri, H. Ian, J. C. Chen, S. Y. Mao, C. C. Chiu, P. Delsing, F. Nori, G.-D. Lin, and I.-C. Hoi, Large collective Lamb shift of two distant superconducting artificial atoms, *Phys. Rev. Lett.* **123**, 233602 (2019).
- [15] A. Carmele, J. Kabuss, F. Schulze, S. Reitzenstein, and A. Knorr, Single photon delayed feedback: A way to stabilize intrinsic quantum cavity electrodynamics, *Phys. Rev. Lett.* **110**, 013601 (2013).
- [16] G. Crowder, J. H. Carmichael, and S. Hughes, Quantum trajectory theory of few-photon cavity-QED systems with a time-delayed coherent feedback, *Phys. Rev. A* **101**, 023807 (2020).
- [17] G. Crowder, L. Ramunno, and S. Hughes, Quantum trajectory theory and simulations of nonlinear spectra and multiphoton effects in waveguide-QED systems with a time-delayed coherent feedback, *Phys. Rev. A* **106**, 013714 (2022).
- [18] G. Crowder, L. Ramunno, and S. Hughes, Improving on-demand single-photon-source coherence and indistinguishability through a time-delayed coherent feedback, *Phys. Rev. A* **110**, L031703 (2024).
- [19] A. B. Young, A. C. T. Thijssen, D. M. Beggs, P. Androvitsaneas, L. Kuipers, J. G. Rarity, S. Hughes, and R. Oulton, Polarization engineering in photonic crystal waveguides for spin-photon entanglers, *Phys. Rev. Lett.* **115**, 153901 (2015).
- [20] T. Lund-Hansen, S. Stobbe, B. Julsgaard, H. Thyrrestrup, T. Sünner, M. Kamp, A. Forchel, and P. Lodahl, Experimental realization of highly efficient broadband coupling of single quantum dots to a photonic crystal waveguide, *Phys. Rev. Lett.* **101**, 113903 (2008).
- [21] N. V. Hauff, H. Le Jeannic, P. Lodahl, S. Hughes, and N. Rotenberg, Chiral quantum optics in broken-symmetry and topological photonic crystal waveguides, *Phys. Rev. Res.* **4**, 023082 (2022).
- [22] M. Mirhosseini, E. Kim, X. Zhang, A. Sipahigil, P. B. Dieterle, A. J. Keller, A. Asenjo-Garcia, D. E. Chang, and O. Painter, Cavity quantum electrodynamics with atom-like mirrors, *Nature* **569**, 692 (2019).
- [23] A. S. Sheremet, M. I. Petrov, I. V. Iorsh, A. V. Poshakin-

- skiy, and A. N. Poddubny, Waveguide quantum electrodynamics: Collective radiance and photon-photon correlations, *Rev. Mod. Phys.* **95**, 015002 (2023).
- [24] A. González-Tudela, V. Paulisch, D. E. Chang, H. J. Kimble, and J. I. Cirac, Deterministic generation of arbitrary photonic states assisted by dissipation, *Phys. Rev. Lett.* **115**, 163603 (2015).
- [25] A. Laucht, S. Pütz, T. Günthner, N. Hauke, R. Saive, S. Frédérick, M. Bichler, M.-C. Amann, A. W. Holleitner, M. Kaniber, and J. J. Finley, A waveguide-coupled on-chip single-photon source, *Phys. Rev. X* **2**, 011014 (2012).
- [26] W. Nie, T. Shi, Y.-x. Liu, and F. Nori, Non-Hermitian waveguide cavity QED with tunable atomic mirrors, *Phys. Rev. Lett.* **131**, 103602 (2023).
- [27] X. Li and L. F. Wei, Designable single-photon quantum routings with atomic mirrors, *Phys. Rev. A* **92**, 063836 (2015).
- [28] A. Asenjo-Garcia, M. Moreno-Cardoner, A. Albrecht, H. J. Kimble, and D. E. Chang, Exponential improvement in photon storage fidelities using subradiance and “selective radiance” in atomic arrays, *Phys. Rev. X* **7**, 031024 (2017).
- [29] A. F. Kockum, G. Johansson, and F. Nori, Decoherence-free interaction between giant atoms in waveguide quantum electrodynamics, *Phys. Rev. Lett.* **120**, 140404 (2018).
- [30] J.-T. Shen and S. Fan, Theory of single-photon transport in a single-mode waveguide. i. coupling to a cavity containing a two-level atom, *Phys. Rev. A* **79**, 023837 (2009).
- [31] S. J. Masson and A. Asenjo-Garcia, Atomic-waveguide quantum electrodynamics, *Phys. Rev. Res.* **2**, 043213 (2020).
- [32] S. Mahmoodian, M. Čepulkovskis, S. Das, P. Lodahl, K. Hammerer, and A. S. Sørensen, Strongly correlated photon transport in waveguide quantum electrodynamics with weakly coupled emitters, *Phys. Rev. Lett.* **121**, 143601 (2018).
- [33] C. W. Gardiner and M. J. Collett, Input and output in damped quantum systems: Quantum stochastic differential equations and the master equation, *Phys. Rev. A* **31**, 3761 (1985).
- [34] J.-T. Shen and S. Fan, Strongly correlated two-photon transport in a one-dimensional waveguide coupled to a two-level system, *Phys. Rev. Lett.* **98**, 153003 (2007).
- [35] J.-T. Shen and S. Fan, Strongly correlated multiparticle transport in one dimension through a quantum impurity, *Phys. Rev. A* **76**, 062709 (2007).
- [36] E. Rephaeli and S. Fan, Few-photon single-atom cavity QED with input-output formalism in fock space, *IEEE Journal of Selected Topics in Quantum Electronics* **18**, 1754 (2012).
- [37] S. Fan, S. E. Kocabaş, and J.-T. Shen, Input-output formalism for few-photon transport in one-dimensional nanophotonic waveguides coupled to a qubit, *Phys. Rev. A* **82**, 063821 (2010).
- [38] Y. Chen, M. Wubs, J. Mørk, and A. F. Koenderink, Coherent single-photon absorption by single emitters coupled to one-dimensional nanophotonic waveguides, *New Journal of Physics* **13**, 103010 (2011).
- [39] K. Barkemeyer, A. Knorr, and A. Carmele, Heisenberg treatment of multiphoton pulses in waveguide QED with time-delayed feedback, *Phys. Rev. A* **106**, 023708 (2022).
- [40] S. Arranz Regidor, G. Crowder, H. Carmichael, and S. Hughes, Modeling quantum light-matter interactions in waveguide QED with retardation, nonlinear interactions, and a time-delayed feedback: Matrix product states versus a space-discretized waveguide model, *Phys. Rev. Res.* **3**, 023030 (2021).
- [41] K. Barkemeyer, A. Knorr, and A. Carmele, Strongly entangled system-reservoir dynamics with multiphoton pulses beyond the two-excitation limit: Exciting the atom-photon bound state, *Phys. Rev. A* **103**, 033704 (2021).
- [42] E. Sánchez-Burillo, J. García-Ripoll, L. Martín-Moreno, and D. Zueco, Nonlinear quantum optics in the (ultra)strong light-matter coupling, *Faraday Discussions* **178**, 335–356 (2015).
- [43] P.-O. Guimond, M. Pletyukhov, H. Pichler, and P. Zoller, Delayed coherent quantum feedback from a scattering theory and a matrix product state perspective, *Quantum Science and Technology* **2**, 044012 (2017).
- [44] S. Mahmoodian, G. Calajó, D. E. Chang, K. Hammerer, and A. S. Sørensen, Dynamics of many-body photon bound states in chiral waveguide QED, *Phys. Rev. X* **10**, 031011 (2020).
- [45] P. Domokos, P. Horak, and H. Ritsch, Quantum description of light-pulse scattering on a single atom in waveguides, *Phys. Rev. A* **65**, 033832 (2002).
- [46] H. T. Dung, L. Knöll, and D.-G. Welsch, Resonant dipole-dipole interaction in the presence of dispersing and absorbing surroundings, *Phys. Rev. A* **66**, 063810 (2002).
- [47] E. Rephaeli, J.-T. Shen, and S. Fan, Full inversion of a two-level atom with a single-photon pulse in one-dimensional geometries, *Phys. Rev. A* **82**, 033804 (2010).
- [48] S. Liu, C. Gustin, H. Liu, X. Li, Y. Yu, H. Ni, Z. Niu, S. Hughes, X. Wang, and J. Liu, Dynamic resonance fluorescence in solid-state cavity quantum electrodynamics, *Nature Photonics* **10**, 1038/s41566-023-01359-x (2024).
- [49] K. Boos, S. K. Kim, T. Bracht, F. Sbresny, J. M. Kaspari, M. Cygorek, H. Riedl, F. W. Bopp, W. Rauhaus, C. Calcagno, J. J. Finley, D. E. Reiter, and K. Müller, Signatures of dynamically dressed states, *Phys. Rev. Lett.* **132**, 053602 (2024).
- [50] S. Arranz Regidor, A. Knorr, and S. Hughes, Theory and simulations of few-photon fock state pulses strongly interacting with a single qubit in a waveguide: exact population dynamics and time-dependent spectra (2024), manuscript in preparation.